ACS APPLIED MATERIALS & INTERFACES

Research Article

www.acsami.org

Highly Sensitive Piezo-Resistive Graphite Nanoplatelet–Carbon Nanotube Hybrids/Polydimethylsilicone Composites with Improved Conductive Network Construction

Hang Zhao and Jinbo Bai*

Laboratoire de Mécanique des Sols, Structures et Matériaux, Ecole Centrale Paris, CNRS UMR8579, PRES UniverSud, Grande Voie des Vignes, 92295 Châtenay-Malabry Cedex, France

Supporting Information

ABSTRACT: The constructions of internal conductive network are dependent on microstructures of conductive fillers, determining various electrical performances of composites. Here, we present the advanced graphite nanoplatelet–carbon nanotube hybrids/polydimethylsilicone (GCHs/PDMS) composites with high piezo-resistive performance. GCH particles were synthesized by the catalyst chemical vapor deposition approach. The synthesized GCHs can be well dispersed in the matrix through the mechanical blending process. Due to the exfoliated GNP and aligned CNTs coupling structure, the flexible composite shows an ultralow percolation threshold (0.64 vol %) and high piezo-resistive sensitivity (gauge factor ~ 10^3 and pressure sensitivity ~ 0.6 kPa^{-1}). Slight motions of finger can be detected and distinguished accurately using the composite film as a typical wearable sensor. These results indicate that designing the internal conductive network could be a reasonable strategy to improve the piezo-resistive performance of composites.

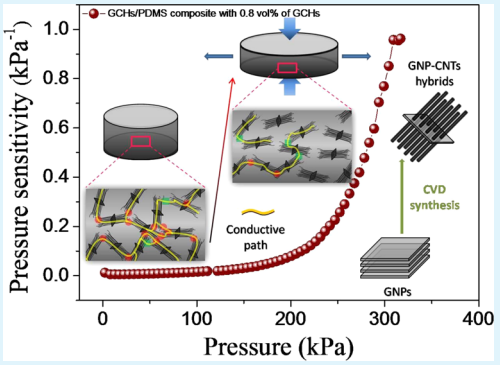

KEYWORDS: *polydimethylsilicone, piezo-resistive pressure sensor, dielectric percolation, conducting composites*

1. INTRODUCTION

Piezo-resistive (PR) materials with merits of being flexible, sensitive, and easy to produce, allowing applied pressure to be quantified through corresponding electrical resistance changes,[1−5] have drawn great interests for their applications in many fields, such as finger sensing, artificial-skin, and wearable electronic devices.[6−12] In order to combine the intrinsic advantage of each component and effectively widen their applications, recently, composing conductive fillers with flexible polymer matrix as composites becomes an efficient approach. According to the percolation theory,[13−16] the typical PR behavior is generally observed at the filler concentration beyond the percolation threshold (f_c), where the formed internal conductive network reconstructs itself synchronously with external applied pressure, showing a measurable electric resistance deviation.

High sensitivity is the key issue of evaluating the PR behavior of composites,[17,18] which can excite more pronounced resistance change response under a slight stimulus. To maintain the flexibility of polymer matrix and design the conductive network reasonably have been considered as effective approaches in improving the PR sensitivity.[19,20] To retain the intrinsic flexibility, a number of studies have focused on decreasing the f_c of composites.[21] In fact, the conductive network structure is strongly dependent on the shape and aspect ratio of fillers.[22−25] The composites with carbon black and metallic particles as zero-dimensional (0D) conductive fillers showed remarkable PR response, owing to their high intrinsic electrical conductivity.[9,26,27] However, to form a conductive network, the high filler loading could inevitably destroy the flexibility of composites. In very recent years, a blooming development made graphene as one of the most popular and competitive nanofillers, due to its extraordinary overall performance.[28−31] Their two-dimensional (2D) structure can substantially increase interfacial adhesion with the matrix and endow the composite with optimized performance.[32] Nevertheless, the difficulty, time, and cost of the composite processing procedure have to be raised by the enormous surface energy of graphene. In our previous report that the alkyl was grafted onto graphene as conductive loading, PDMS based composites showed high sensitivity and low f_c.[33] Whereas, much solvent was utilized which limited the possibility of industrial-scale production in short-term. Graphite nanoplatelets (GNPs) served as another type of 2D filler, composing of tens of natural flake graphite sheets, have endowed the composites with excellent performances in recent researches.[8,34−36] However, it is believed that their functionality could be further improved by exfoliating GNPs into individual GNP layers. Among these conductive fillers, carbon nanotubes (CNTs) have been most intensively studied because of their

Received: February 13, 2015
Accepted: April 21, 2015
Published: April 21, 2015

DOI: 10.1021/acsami.5b01413
ACS Appl. Mater. Interfaces 2015, 7, 9652−9659

typical one-dimensional (1D) structure with high aspect ratio and outstanding intrinsic properties.[37−42] But how to solve the problem that CNTs are easily frizzy and entangled in the polymer matrix is a long-term challenge. It is worthy to mention that the high aspect ratio structure of CNTs could lead to opposite influences on reducing the f_c and enhancing the PR sensitivity, respectively.[22,24] On one hand, it has been proved that the percolation threshold is inversely proportional to aspect ratio. On the other hand, in contrast to the CNTs with high aspect ratio, the counterparts with low aspect ratio prefer to orientate with the deformation; hence, their composites would show higher sensitivity to external stimulus.

To overcome these problems, a special coupling micro-architecture of GNP−CNT hybrids (GCHs) was synthesized through the approach of catalyst chemical vapor disposition (CCVD).[43] Different from other CNT−substrate hybrid structures, GCHs served as the distinctive conductive filler with features of all-carbon composition, in particular coupling structure and low intrinsic density. After a series of processes of carbon source decomposition and carbon atoms redisposition, numerous CNTs can well grow and vertically align onto the surfaces of GNP substrates, forming the special structure.[43−45] Especially, GNP substrates are capable of working as the "wire concentrators" or "transport hubs", connecting with all the conductive single CNTs as "sideways" directly. These electrical conductive "hub" structures could effectively promote the interconnection among hybrids and facilitate the formation of a conductive network. In addition, the PR behavior of a composite based on micronano-hybrids has rarely been reported, particularly for the all-carbon GCHs loaded composite.

Polydimethylsilicone (PDMS) that utilized as the flexible matrix of PR composite has received wide attention and great approval, due to its excellent thermal stability, fast response speed, high elastic elasticity, easy production, and low cost.[46] Notably, the particular biocompatibility of PDMS could benefit the potential application as artificial skin.[47]

In this study, we present the advanced GCHs/PDMS composites with high PR performance, prepared through mechanical blending GCHs with PDMS matrix using the three-roll mill at room temperature. The GCHs particles with 1D−2D coupling structure were precisely synthesized by CCVD approach. The mechanical blending process without chemical solvent can not only keep the hybrid structure from breaking but also provide an excellent interfacial adhesion with matrix. An ultralow percolation threshold and the significant positive PR behavior with high sensitivity and stability were achieved. In addition, the result of the typical finger-sensing experiment indicates that the route of designing conductive network to improve the PR performance of flexible composite is reasonable. The GCHs/PDMS composite could be potentially applied as artificial skin with high PR performances.

2. EXPERIMENTAL SECTION

Preparation of the GNP−CNTs Hybrids and Composites. Graphite nanoplatelets hundreds of nanometers in thickness and 4−5 μm in diameter were provided by Xiamen K-Nano Graphene Technology Co. The hydroxyl-terminated PDMS (50 000 mPa·s, from Sigma-Aldrich) was chosen as the flexible insulating elastomer matrix in our experiment.

The GCH particles were synthesized through the floating-catalyst CVD method without any pretreatment. Acetylene C_2H_2 and xylene $C_6H_4(CH_3)_2$ were selected as cocarbon sources, and ferrocene $Fe(C_5H_5)_2$ served as catalyst precursor for the growth of vertically aligned CNTs on the GNP surface. The synthesis time and temperature were fixed as 10 min and 650 °C, respectively, in order to achieve the hybrid architecture with the CNT/GNP mass ratio approximated to 1:1. The mixing process of the GCHs/PDMS nanocomposite was done using a three-roll mill (EXAKT 80, Germany) at room temperature, with the hybrid volume fraction ranging from 0 to 1.5 vol %. A long mixing time (45 min) and a low mixing shearing rate (50 rpm) were used for not only obtaining an excellent dispersion but also keeping the hybrid architecture from being damaged caused by an overstrong mechanical shear as much as possible. Then, the curing agent tetraethyl orthosilicate and an accelerant dibutyltindilaurate (both from Sigma-Aldrich) were added into the mixture. The resulting composite was poured out into a metal mold and cured under a compression of 100 bar, at room temperature. The final disk-shape samples with diameter of 10 mm and thickness of 3 mm were prepared for uniaxial compression. The rectangle film samples with area of 10 × 80 mm^2 and thickness of 150 μm were prepared for finger sensing.

General Characterization. Scanning electron microscope (ZEISS LEO 1530 Gemini) was used to observe the morphology of the fillers and the fractured surfaces of GCHs/PDMS composite. The dielectric performances were evaluated in the frequency range of 10^3−10^6 Hz using an impedance analyzer (Solartron 1260). X-ray diffraction (XRD) patterns of the GCHs/PDMS composites were measured on XRD detector (BRUKER D2 PHASER with X Flash 430).

Real-Time Piezoresistivity Testing. The real-time piezoresistivity tests were carried out on a combination of a universal testing machine (Instron 5544) and an electrometer (Keithley 2400). Loading−unloading compression cyclic operation with a constant crosshead rate of 1 mm/min and the measurement of volume electrical resistance by the two-probe method were performed, respectively. To reduce the contact resistance, Pt electrodes were coated onto both sides of the samples through the plasma sputtering approach prior to the measurement. The electrical performance data were recorded through a LabVIEW program.

3. RESULTS AND DISCUSSION

Scheme 1 illustrates the main fabrication process of GCHs/PDMS composites. The structure of the GNP substrates is

Scheme 1. Schematic Illustration of the Preparation of GCH Particles and GCHs/PDMS Composites

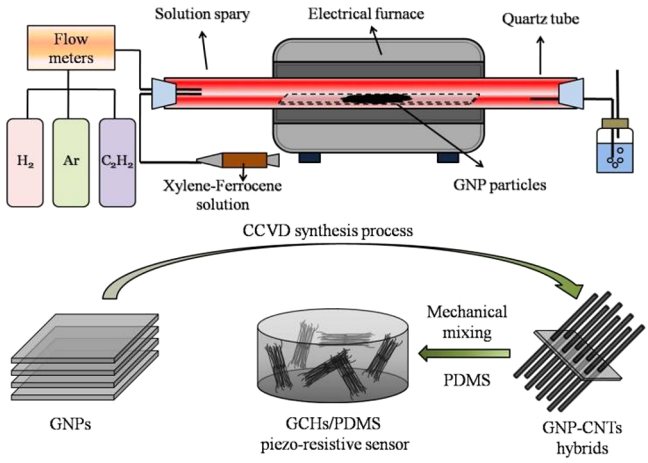

demonstrated in Figure 1a, with an average thickness of hundreds of nanometers and diameter of 1−4 μm, respectively. Figure 1b clearly shows the 1D−2D coupling structure of the synthesized GCHs, where the length and diameter of those vertically aligned CNTs are 2−4 μm and 15−20 nm, respectively. The structure of the hybrids can be tuned through controlling the experimental parameters of CVD process.

DOI: 10.1021/acsami.5b01413
ACS Appl. Mater. Interfaces 2015, 7, 9652−9659

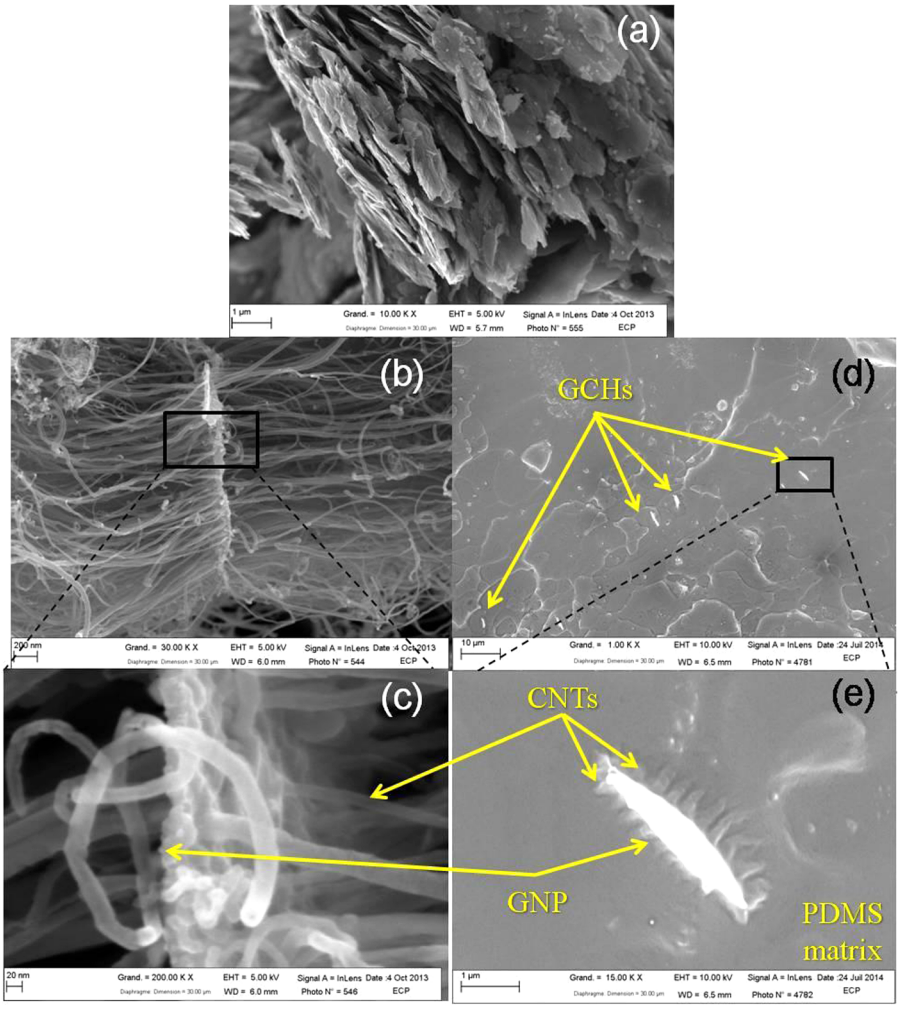

Figure 1. Typical morphological characterization using SEM: (a) the structure of GNPs and (b and c) the structure of GCHs particles. (d) SEM image of the fracture surface of the GCHs/PDMS composite. (e) High-magnification image of GCH particle well embedded in the matrix.

Aligning CNTs onto certain substrates has been used for a potential strategy to avoid CNT entanglement.[48,49] It is noteworthy that all CNT clusters were observed to grow perpendicularly onto the surfaces of individual GNP rather than those of GNP aggregates (natural state) (see Figure 1c). In fact, during the CVD synthesis process of GCHs, the high temperature in the furnace was used for not only offering required energy for chemical reaction but also accompanying a thermal exfoliation effect which separates the original GNP aggregates into a number of much thinner individual GNP layers. Thus, both the specific surface area of fillers and the interfical area between fillers and the polymer matrix can be increased effectively. Several notable properties of the composite are well endowed by this special structure, which will be introduced in detail in the following paragraphs.

Both the fillers distribution and the interfacial condition between fillers and matrix play crucial roles in evaluating the stability of composites. Figure 1d shows the SEM morphology of the fractured surface of the GCHs/PDMS composite, where GCHs are well distributed in the soft PDMS matrix without aggregation. The 1D−2D coupling structure displays the maximum effective surface, leading to a largely augmented interfacial adhesion. Furthermore, the individual CNTs are bonded on the GNP substrate and separated from each other by the insulating PDMS matrix, forming the conductive "hub" structure. The "hub" structure can be embedded tightly in PDMS matrix without an obvious break (see Figure 1e), which makes GCHs/PDMS composite scalable from laboratory to industrial scale.

In order to further investigate the thermal exfoliating effect of GNPs, Figure 2 provides the X-ray diffraction (XRD) patterns of CNTs, GNPs aggregate, and the GNP−CNTs hybrid. From GNPs to GCHs, the strong peak around 26.46° dropped

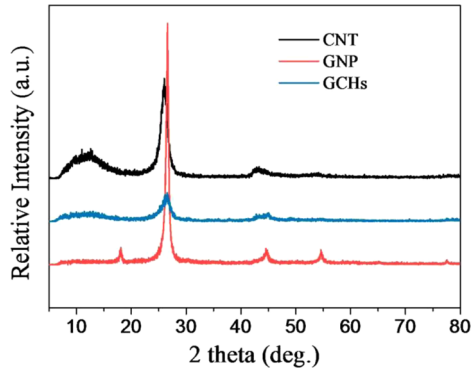

Figure 2. X-ray diffraction patterns of CNTs, GNPs aggregate, and the GCH particles.

DOI: 10.1021/acsami.5b01413
ACS Appl. Mater. Interfaces 2015, 7, 9652−9659

significantly, indicating the interlayer distance of exfoliated GNP substrate kept constant, but the exfoliation degree of GNPs aggregate enhanced. However, the sharp peaks at 44° and 54.3° of the GNPs aggregate became gradual, which is in accordance with typical peaks of CNTs, suggesting that the CNT clusters were grown onto the surface of GNP substrate.

The dielectric percolation effect is one of the most important signals of forming the conductive network; hence, the dielectric performance of the GCHs/PDMS composite was characterized. Figure 3 demonstrates the dependence of AC conductivity

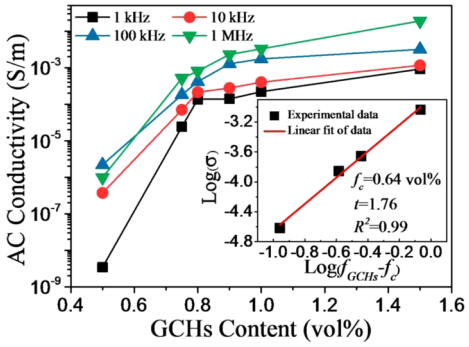

Figure 3. AC conductivity of the GCHs/PDMS composites with different GCHs loading at room temperature. The inset shows the best fit of $\log(\sigma)$ vs $\log(f_{GCHs} - f_c)$.

(σ_{AC}) of GCHs/PDMS composite on filler concentrations at the frequency range of 1 kHz−1 MHz, from which an obvious percolation transition from insulating ($\sigma_{AC} \sim 10^{-9}$ S m^{-1}) to conducting ($\sigma_{AC} \sim 10^{-2}$ S m^{-1}) with the increasing GCHs loading can be noticed. Notably, more than 4 orders of magnitude rise of σ_{AC} can be achieved under the range of GCHs loading from 0.5 to 0.9 vol %, illustrating the constructing process of the inner conductive network. The conductivity of composite that approaches the percolation threshold can be evaluated using the following power law:[36]

$$\sigma \propto (f_{GCHs} - f_c)^t \qquad \text{for } f_{GCHs} > f_c \tag{1}$$

where f_{GCHs} and f_c are the volume fraction of conductive GCHs particles and the percolation threshold of the composite, respectively, and t is the critical exponent in the conducting region. The best fits of the experimental conductivity values to the log−log plots of the power laws provides f_c = 0.64 vol % (see the inset in Figure 3). The critical exponent in the conducting region, t = 1.76, is in accord with the universal values ($t \approx 1.6$–2) for the composite loading three-dimensional conductive fillers from the percolation theory.[16] It is worthy to note that such low percolation value was rarely reported in most PDMS-based composites using the carbon series materials as conductive filler. It is mainly ascribed to these fully conductive multiple-branching "hub" structures, which can not only enhance the interfacial area and polarization but also extend their effective contacting space. Thus, the construction of an internal conductive network was facilitated effectively.

To study the relationship between PR behavior and the GCHs loading under relevantly low stimulus, the maximum applied pressure was restricted to 0.32 MPa. The resistance change (R/R_0)−pressure curves averaged from more than three independent tests are depicted in Figure 4a. A stepwise compression (1 mm/min) was applied to the disk-shape samples until the maximum charge. A series of positive pressure

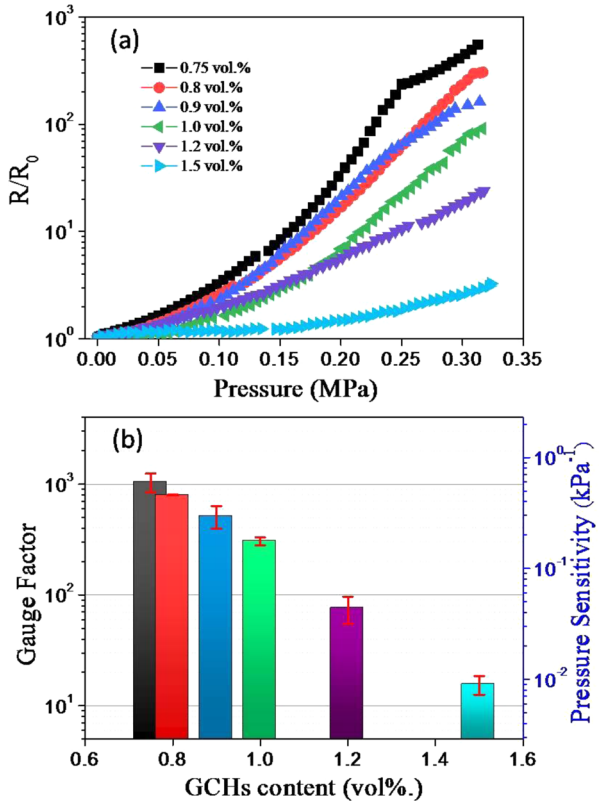

Figure 4. (a) Typical PR behaviors variation and (b) piezo-resistive sensitiviy of GCHs/PDMS composites with various GCHs loading under uniaxial compression.

dependence of resistance can be observed for all tested GCHs loading. Noteworthy, the composites with filler concentrations in the vicinity of the percolation threshold show larger resistance changes under the same pressures than those with much higher filler concentration. Due to the particular conductive structure of the CGHs, the sensitive conductive network can be formed at such low concentration via the tunneling effect.[8,50,51] However, with increasing filler content, the connection mode of the conductive network transfers from the tunneling state to the filler overlapping state, in which there is enough quantity of GCHs to overlap each other. Thus, the inner conductive network becomes relatively stable and insensitive to external stimulus.

Generally, the sensitivity of strain sensors and pressure sensors can be evaluated by the gauge factor (GF) and pressure sensitivity (PS), respectively.[35]

$$\text{GF} = \frac{\Delta R/R_0}{\Delta l/l_0} = \frac{\Delta R/R_0}{\varepsilon} \tag{2}$$

$$\text{PS} = \frac{\Delta R/R_0}{P} \tag{3}$$

where R_0 is the nominal resistance in the unloaded state (pressure and strain are equal to 0), ΔR is the resistance change, l_0 and Δl are the original thickness of sensor sample in the unloaded state and the thickness change, respectively, and p is applied pressure. The dependence of GF and PS values, calculated by the average during the cyclic tests without the first cycle, on filler concentrations is illustrated in Figure 4b. Similar to the AC conductivity, both GF and PS values decrease with the increasing filler content. Especially, an outstanding

DOI: 10.1021/acsami.5b01413
ACS Appl. Mater. Interfaces 2015, 7, 9652−9659

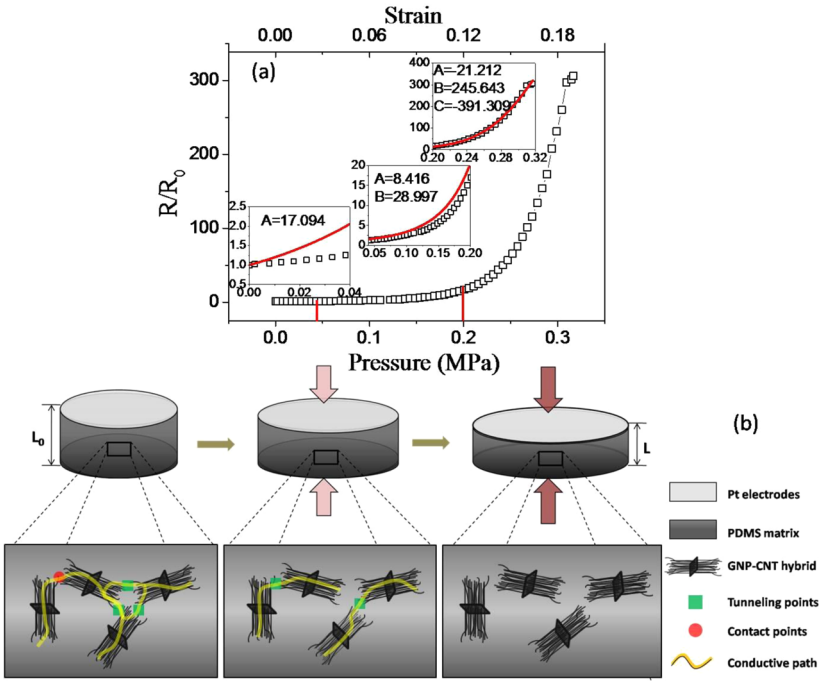

Figure 5. (a) Resistance change on the applied pressure and strain of GCHs/PDMS composite with 0.8 vol %. GCHs. The inset images show the three-step theoretical fit of experimental data. (b) Schematic diagram of the dependence between the internal conductive network structure and the external applied pressure of three steps.

sensitivity (GF ~ 10^3, PS ~ 0.6 kPa^{-1}) can be achieved from the sample with the GCHs content of 0.75 vol % under the pressure of 0.32 MPa. This result is adequately competitive among reported carbon filler/PDMS composites. Thanks to the "hub" structure, on one hand, one GCH particle can be totally activated and conducted by another through even just a one-point contact or weak tunneling effect that takes place on any single CNT of GCHs. On the other hand, the relatively low percolation threshold could well retain the flexibility of the PDMS matrix for the composite, allowing a large deformation under small pressure. Therefore, the composite is greatly sensitive to the applied pressure.

By reason for its stable performance, the sample with 0.8 vol % GCHs was chosen to study the piezo-resistive behavior of the GCHs/PDMS composite in detail (see Figure 5a). On the basis of the influences on conductive network that induced by the increasing external pressure, the piezo-resistance correlation can be devided into three parts. A sequence of exponential fittings were made for each part, according to the modified formulas that derived from the tunneling effect[8] (see the insets in Figure 5a). The detailed fitting process is shown in the Supporting Information. Figure 5b illustrates schematically the inner conductive network constructions for three parts, respectively.

First, the fully conductive network is mainly made up via the tunneling effect among fillers.[50] A tiny resistance change can be observed under the applied pressure from 0 to 0.04 MPa. Hence, we call the first part a "tunneling state". Due to the influence of applied pressure to the reorientation of fillers being slight, the correlation of piezo-resistive behavior of this part is as follows:

$$R/R_0 = (1 + p)\exp(Ap) \tag{4}$$

p is applied pressure that is proportional to strain, and A is the parameter relevant to the intrinsic properties of materials and deformation.[8]

When the applied pressure increases to 0.04−0.2 MPa, this range is defined as a "transitional state". In this state, GCH particles begin to move and reorientate with the deformation of the PDMS matrix. Some initial contacting joints loosen, and others are separated. The former ones continue connecting the circuit to keep the functionality of the conductive network through the tunneling effect. However, the latter ones are responsible for the partial break of the conductive paths. Therefore, the resistance of composite exhibits a measurable enhancement. The relationship between R/R_0 and the pressure can be fitted as follows:[8]

$$R/R_0 = (1 + p)\exp(Ap + Bp^2) \tag{5}$$

where B and C are both constants.

With the further increasing pressure, more intense reorientation takes place. The distance between two GCHs becomes beyond the tunnel distance. Plenty of GCHs are separated by the continuous and insulating PDMS matrix, resulting in the "discontinuous state". Due to the special network construction, a small reorientation of GCHs might result in a huge role transformation from the "transport hubs" to the "isolated islet", subsequently damaging the conductive network. Hence, the composite with GCHs as conductive units is more sensitive to the applied pressure. The modified function used to fit PR behavior is

$$R/R_0 = (1 + p)\exp(Ap + Bp^2 + Cp^3) \tag{6}$$

Besides high sensitivity, rapid electrical resistance response and excellent repeatability are also considered as critical properties of ideal piezo-resistive materials.[33] To detect the dynamic synchrony between the cyclic pressure and corresponding resistance change, the multicycle piezo-resistive tests were done to the sample with 0.8 vol % GCHs. An excellent real-time response with little hysteresis and shoulder peak was noticed in Figure 6a. Although a distinct piezo-resistive

DOI: 10.1021/acsami.5b01413
ACS Appl. Mater. Interfaces 2015, 7, 9652−9659

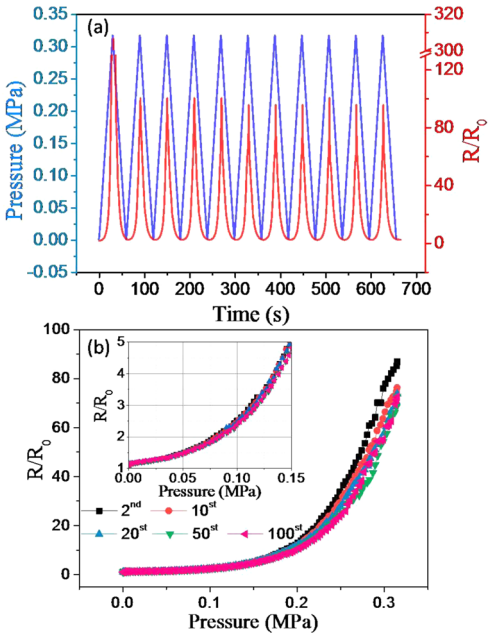

Figure 6. (a) Relative resistance (R/R_0) and applied pressure vs time under periodic loading−unloading tests; (b) (R/R_0) under 100 loading−unloading cycles with the pressure ranging from 0 to 0.31 MPa. The inset shows the consistent PR response under 100 loading−unloading cycles with the small applied pressure ranging from 0 to 0.15 MPa.

response at the first cycle was observed resulting from the Mullins effect,[52] the stable and excellent resistance changes (R/R_0 > 90) can be achieved in the following 10 cycles. An excellent repeatability is a decisive property for practical application. Figure 6b shows that the long-term PR behavior of the composite with 0.8 vol % GCHs during 100 loading−unloading cycles under the pressure range (0−0.32 MPa). Although the value of R/R_0 can be stably maintained over 70, there was a small decline of maximun resistance change and a slight augmentation of minimum resistance change shown after a high number of cycles. This could be interpreted by the structure of the conductive networks being permanently modified by a long-term periodic loading−unloading process.[42] Besides, in the range of ultralow stimulus (lower than 0.1 MPa) the piezo-resistive response tends to provide an excellent consistency (see the inset of Figure 6b).

To achieve the promising functionalities of artificial skin such as human−machine interaction and motion recognition, the typical GCHs/PDMS composite film finger sensor was fabricated using a similar preparation process. The film finger sensor was fixed onto the surface of the stretchable nitrile glove. Silver paste was coated between the film finger sensor and the ultrathin conductive wire (used for reducing the contact disturbance induced by movement) to reduce the contact resistance (watch the Supporting Information video). As illustrated in Figure 7a, we considered the relaxing straight index finger as the initial state, and the collected electrical signals were the baseline. In Figure 7b−d, three simple motions were chosen to evaluate the response performance of the film finger sensor: A, B, and C are the motions of bending the second joint and third joint of the index finger and clenching, respectively. Moreover, the tension deformation amplitudes of these motions were calculated as 16.9%, 20.5%, and 28.9%, respectively. Figure 7e shows the distinctive real-time resistance

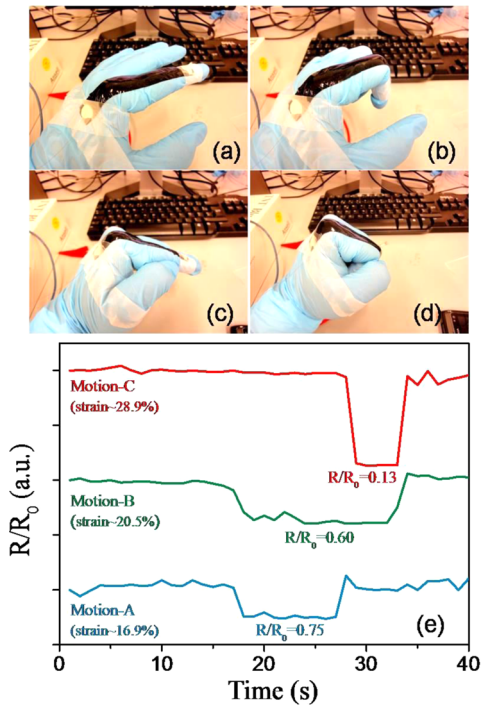

Figure 7. GCHs/PDMS composite film serving as a finger movement detector. (a) Photograph of the relaxing state of the finger. (b−d) Photographs of three distinct motions (A, B, and C) of bending the second joint and the third joint of index finger and clenching, respectively. (e) Relative resistance changes for each independent movement.

changes (R/R_0 of motions A, B, and C are 0.75, 0.6, and 0.13, respectively) and their unique duration times, which are perfectly in accordance with the different amplitudes of motions and corresponding action times. A particularly negative piezo-resistance response under tension deformations was revealed, which may result from it being difficult for GCHs to orientate along the thickness direction during the pressure-casting process, especially for film samples. With the enhanced tension strain, GCHs prefer reorientating near the tension direction. The anisotropic degree increases correspondingly, and the tunneling effect may take place more easily. Therefore, the composite film finger sensor that uses GCHs as conductive filler can not only respond to subtle actions but also distinguish them accurately, which makes the composite a good candidate for artificial skin and wearable pressure sensor applications.

4. CONCLUSIONS

In conclusion, the advanced GCHs/PDMS flexible composites with excellent PR behavior are prepared. The typical 1D−2D coupling GCHs structure is synthesized through the CCVD approach, in which GNP aggregates can be effectively exfoliated to offer substrates for growing the vertically aligned CNTs. Good dispersion and excellent interfacial adhesion can be achieved by the mechanical mixing process. According to the percolation theory, the composite shows a significant increase of AC conductivity with filler loading. An ultralow percolation threshold (0.64 vol %) is achieved due to the "hub" structure of conductive units. Moreover, the modified three-step theoretical exponential fit can well account for the more sensitive positive PR behavior of composite under uniaxial compression. Beyond the threshold, the PR sensitivity is inversely proportional to the

DOI: 10.1021/acsami.5b01413
ACS Appl. Mater. Interfaces 2015, 7, 9652−9659

GCHs content. Especially, the composite with 0.75 vol % GCHs displays such extraordinary sensitivity that the GF and PS value are as high as 10^3 and 0.6 kPa^{-1}, respectively. During the cyclic compression loading, the PR behavior of composites manifests a superior dynamic correspondence with applied pressure. In the meantime, the resistance response can retain at a relatively high level after 100 loading−unloading cycles. Notably, the typical finger-sensing experiment indicates that the GCHs/PDMS composites are competent to detect and even distinguish the slight finger motions. In summary, the strategy of the conductive network design will contribute to the development of PR composites with higher performances and further drive the fabrication process to industrial scale.

■ ASSOCIATED CONTENT

Supporting Information

This material includes the detailed fitting process and three figures of TGA-DSC data, schematic construction of the "hub" structure, piezo-resistive behavior under small charge of GCHs/PDMS composites; two figures of morphological image and electrical property of GNPs/CNTs/PDMS three-phase composites; and three tables of calculated parameters and the comparison among similar reports. Movie showing GCHs/PDMS composite film serving to detect finger movements. The Supporting Information is available free of charge on the ACS Publications website at DOI: 10.1021/acsami.5b01413.

■ AUTHOR INFORMATION

Corresponding Author

*E-mail: jinbo.bai@ecp.fr. Tel./Fax: +33(0)141131316.

Notes

The authors declare no competing financial interest.

■ ACKNOWLEDGMENTS

Authors are grateful to Mrs. F. Garnier, Dr. D. Salem, and Dr. L.Belkadi for the SEM investigations and Mr. XF Bai for the XRD measurements. H.Z. also gratefully acknowledges the financial support of China Scholarship Council.

■ REFERENCES

(1) He, R.; Yang, P. Giant Piezoresistance Effect in Silicon Nanowires. *Nat. Nanotechnol.* **2006**, *1* (1), 42−46.

(2) Hammock, M. L.; Chortos, A.; Tee, B. C.; Tok, J. B.; Bao, Z. 25th Anniversary Article: The Evolution of Electronic Skin (E-skin): A Brief History, Design Considerations, and Recent Progress. *Adv. Mater.* **2013**, *25* (42), 5997−6038.

(3) Benight, S. J.; Wang, C.; Tok, J. B. H.; Bao, Z. Stretchable and Self-healing Polymers and Devices for Electronic Skin. *Prog. Polym. Sci.* **2013**, *38* (12), 1961−1977.

(4) Stassi, S.; Cauda, V.; Canavese, G.; Pirri, C. F. Flexible Tactile Sensing Based on Piezoresistive Composites: A Review. *Sensors* **2014**, *14* (3), 5296−332.

(5) Carmona, F.; Canet, R.; Delhaes, P. Piezoresistivity of Heterogeneous Solids. *J. Appl. Phys.* **1987**, *61* (7), 2550.

(6) Ramuz, M.; Tee, B. C.; Tok, J. B.; Bao, Z. Transparent, Optical, Pressure-sensitive Artificial Skin for Large-area Stretchable Electronics. *Adv. Mater.* **2012**, *24* (24), 3223−3227.

(7) Sekitani, T.; Someya, T. Stretchable, Large-area Organic Electronics. *Adv. Mater.* **2010**, *22* (20), 2228−2246.

(8) Chen, L.; Chen, G. H.; Lu, L. Piezoresistive Behavior Study on Finger-sensing Silicone Rubber/Graphite Nanosheet Nanocomposites. *Adv. Funct. Mater.* **2007**, *17* (6), 898−904.

(9) Canavese, G.; Stassi, S.; Fallauto, C.; Corbellini, S.; Cauda, V.; Camarchia, V.; Pirola, M.; Pirri, C. F. Piezoresistive Flexible Composite for Robotic Tactile Applications. *Sens. Actuators, A* **2014**, *208*, 1−9.

(10) Castano, L. M.; Flatau, A. B. Smart Fabric Sensors and E-textile Technologies: A Review. *Smart Mater. Struct.* **2014**, *23* (5), 053001.

(11) Li, L. W. a. Y. A Review for Conductive Polymer Piezoresistive Composites and a Development of a Compliant Pressure Transducer. *IEEE Trans. Instrum. Meas.* **2013**, *62*, 8.

(12) Kong, J. H.; Jang, N. S.; Kim, S. H.; Kim, J. M. Simple and Rapid Micropatterning of Conductive Carbon Composites and Its Application to Elastic Strain Sensors. *Carbon* **2014**, *77*, 199−207.

(13) Dang, Z. M.; Wang, L.; Yin, Y.; Zhang, Q.; Lei, Q. Q. Giant Dielectric Permittivities in Functionalized Carbon-Nanotube/ Electroactive-Polymer Nanocomposites. *Adv. Mater.* **2007**, *19* (6), 852−857.

(14) Nan, C. W.; Shen, Y.; Ma, J. Physical Properties of Composites Near Percolation. *Annu. Rev. Mater. Res.* **2010**, *40* (1), 131−151.

(15) Yuan, J.-K.; Yao, S.-H.; Dang, Z.-M.; Sylvestre, A.; Genestoux, M.; Bai, J. Giant Dielectric Permittivity Nanocomposites: Realizing True Potential of Pristine Carbon Nanotubes in Polyvinylidene Fluoride Matrix through an Enhanced Interfacial Interaction. *J. Phys. Chem. C* **2011**, *115* (13), 5515−5521.

(16) Dang, Z. M.; Yuan, J. K.; Zha, J. W.; Zhou, T.; Li, S. T.; Hu, G. H. Fundamentals, Processes and Applications of High-permittivity Polymer Matrix Composites. *Prog. Mater. Sci.* **2012**, *57* (4), 660−723.

(17) Lin, L.; Liu, S.; Zhang, Q.; Li, X.; Ji, M.; Deng, H.; Fu, Q. Towards Tunable Sensitivity of Electrical Property to Strain for Conductive Polymer Composites Based on Thermoplastic Elastomer. *ACS Appl. Mater. Interfaces* **2013**, *5* (12), 5815−24.

(18) Laukhina, E.; Pfattner, R.; Ferreras, L. R.; Galli, S.; Mas-Torrent, M.; Masciocchi, N.; Laukhin, V.; Rovira, C.; Veciana, J. Ultrasensitive Piezoresistive All-organic Flexible Thin Films. *Adv. Mater.* **2010**, *22* (9), 977−81.

(19) Hu, N.; Karube, Y.; Arai, M.; Watanabe, T.; Yan, C.; Li, Y.; Liu, Y.; Fukunaga, H. Investigation on Sensitivity of A Polymer/Carbon Nanotube Composite Strain Sensor. *Carbon* **2010**, *48* (3), 680−687.

(20) Deng, H.; Lin, L.; Ji, M.; Zhang, S.; Yang, M.; Fu, Q. Progress on The Morphological Control of Conductive Network in Conductive Polymer Composites and the Use as Electroactive Multifunctional Materials. *Prog. Polym. Sci.* **2014**, *39* (4), 627−655.

(21) Dang, Z. M.; Yuan, J. K.; Yao, S. H.; Liao, R. J. Flexible Nanodielectric Materials with High Permittivity for Power Energy Storage. *Adv. Mater.* **2013**, *25* (44), 6334−6365.

(22) Cattin, C.; Hubert, P. Piezoresistance in Polymer Nanocomposites with High Aspect Ratio Particles. *ACS Appl. Mater. Interfaces* **2014**, *6* (3), 1804−11.

(23) Shehzad, K.; Dang, Z.-M.; Ahmad, M. N.; Sagar, R. U. R.; Butt, S.; Farooq, M. U.; Wang, T.-B. Effects of Carbon Nanotubes Aspect Ratio on The Qualitative and Quantitative Aspects of Frequency Response of Electrical Conductivity and Dielectric Permittivity in The Carbon Nanotube/Polymer Composites. *Carbon* **2013**, *54*, 105−112.

(24) Jiang, M.-J.; Dang, Z.-M.; Xu, H.-P.; Yao, S.-H.; Bai, J. Effect of Aspect Ratio of Multiwall Carbon Nanotubes on Resistance-Pressure Sensitivity of Rubber Nanocomposites. *Appl. Phys. Lett.* **2007**, *91* (7), 072907.

(25) Knaapila, M.; Hoyer, H.; Kjelstrup-Hansen, J.; Helgesen, G. Transparency Enhancement for Photoinitiated Polymerization (UV Curing) through Magnetic Field Alignment in A Piezoresistive Metal/Polymer Composite. *ACS Appl. Mater. Interfaces* **2014**, *6* (5), 3469−76.

(26) Luheng, W.; Tianhuai, D.; Peng, W. Influence of Carbon Black Concentration on Piezoresistivity for Carbon-Black-Filled Silicone Rubber Composite. *Carbon* **2009**, *47* (14), 3151−3157.

(27) Zhou, J. F.; Song, Y. H.; Zheng, Q.; Wu, Q.; Zhang, M. Q. Percolation Transition and Hydrostatic Piezoresistance for Carbon Black Filled Poly(Methylvinylsilioxane) Vulcanizates. *Carbon* **2008**, *46* (4), 679−691.

(28) Geim, A. K.; Novoselov, K. S. The Rise of Graphene. *Nat. Mater.* **2007**, *6* (3), 183−191.

(29) Yan, C.; Wang, J.; Kang, W.; Cui, M.; Wang, X.; Foo, C. Y.; Chee, K. J.; Lee, P. S. Highly Stretchable Piezoresistive Graphene-

DOI: 10.1021/acsami.5b01413
ACS Appl. Mater. Interfaces 2015, 7, 9652−9659

nanocellulose Nanopaper for Strain Sensors. *Adv. Mater.* **2014**, *26* (13), 2022−7.
(30) Zhu, S.-E.; Krishna Ghatkesar, M.; Zhang, C.; Janssen, G. C. A. M. Graphene Based Piezoresistive Pressure Sensor. *Appl. Phys. Lett.* **2013**, *102* (16), 161904.
(31) Bae, S.-H.; Lee, Y.; Sharma, B. K.; Lee, H.-J.; Kim, J.-H.; Ahn, J.-H. Graphene-based Transparent Strain Sensor. *Carbon* **2013**, *51*, 236−242.
(32) Stankovich, S.; Dikin, D. A.; Dommett, G. H.; Kohlhaas, K. M.; Zimney, E. J.; Stach, E. A.; Piner, R. D.; Nguyen, S. T.; Ruoff, R. S. Graphene-based Composite Materials. *Nature* **2006**, *442* (7100), 282−286.
(33) Hou, Y.; Wang, D.; Zhang, X.-M.; Zhao, H.; Zha, J.-W.; Dang, Z.-M. Positive Piezoresistive Behavior of Electrically Conductive Alkyl-functionalized Graphene/Polydimethylsilicone Nanocomposites. *J. Mater. Chem. C* **2013**, *1* (3), 515.
(34) Luo, S.; Liu, T. SWCNT/Graphite Nanoplatelet Hybrid Thin Films for Self-Temperature-Compensated, Highly Sensitive, and Extensible Piezoresistive Sensors. *Adv. Mater.* **2013**, *25* (39), 5650−5657.
(35) Lee, C.; Jug, L.; Meng, E. High Strain Biocompatible Polydimethylsiloxane-based Conductive Graphene and Multiwalled Carbon Nanotube Nanocomposite Strain Sensors. *Appl. Phys. Lett.* **2013**, *102* (18), 183511.
(36) He, F.; Lau, S.; Chan, H. L.; Fan, J. High Dielectric Permittivity and Low Percolation Threshold in Nanocomposites Based on Poly(Vinylidene Fluoride) and Exfoliated Graphite Nanoplates. *Adv. Mater.* **2009**, *21* (6), 710−715.
(37) Iijima, S. Helical Microtubules of Graphitic Carbon. *Nature* **1991**, *354* (6348), 56−58.
(38) Coleman, J. N.; Khan, U.; Blau, W. J.; Gun'ko, Y. K. Small but Strong: A Review of The Mechanical Properties of Carbon Nanotube−Polymer Composites. *Carbon* **2006**, *44* (9), 1624−1652.
(39) Thostenson, E. T.; Chou, T. W. Carbon Nanotube Networks: Sensing of Distributed Strain and Damage for Life Prediction and Self Healing. *Adv. Mater.* **2006**, *18* (21), 2837−2841.
(40) Wang, L.; Cheng, L. Piezoresistive Effect of A Carbon Nanotube Silicone-matrix Composite. *Carbon* **2014**, *71*, 319−331.
(41) Li, C.; Thostenson, E. T.; Chou, T.-W. Sensors and Actuators Based on Carbon Nanotubes and Their Composites: A Review. *Compos. Sci. Technol.* **2008**, *68* (6), 1227−1249.
(42) Cravanzola, S.; Haznedar, G.; Scarano, D.; Zecchina, A.; Cesano, F. Carbon-based Piezoresistive Polymer Composites: Structure and Electrical Properties. *Carbon* **2013**, *62*, 270−277.
(43) Dichiara, A.; Yuan, J.-K.; Yao, S.-H.; Sylvestre, A.; Bai, J. Chemical Vapor Deposition Synthesis of Carbon Nanotube-Graphene Nanosheet Hybrids and Their Application in Polymer Composites. *J. Nanosci. Nanotechnol.* **2012**, *12* (9), 6935−6940.
(44) He, D.; Bozlar, M.; Genestoux, M.; Bai, J. Diameter- and Length-dependent Self-Organizations of Multi-walled Carbon Nanotubes on Spherical Alumina Microparticles. *Carbon* **2010**, *48* (4), 1159−1170.
(45) He, D.; Li, H.; Li, W.; Haghi-Ashtiani, P.; Lejay, P.; Bai, J. Growth of Carbon Nanotubes in Six Orthogonal Directions on Spherical Alumina Microparticles. *Carbon* **2011**, *49* (7), 2273−2286.
(46) Zhao, H.; Wang, D.-R.; Zha, J.-W.; Zhao, J.; Dang, Z.-M. Increased Electroaction through A Molecular Flexibility Tuning Process in TiO2−Polydimethylsilicone Nanocomposites. *J. Mater. Chem. A* **2013**, *1* (9), 3140.
(47) Mannsfeld, S. C. B.; Tee, B. C.-K.; Stoltenberg, R. M.; Chen, C. V. H.-H.; Barman, S.; Muir, B. V. O.; Sokolov, A. N.; Reese, C.; Bao, Z. Highly Sensitive Flexible Pressure Sensors with Microstructured Rubber Dielectric. *Nat. Mater.* **2010**, *9*, 859−864.
(48) Yuan, J.-K.; Li, W.-L.; Yao, S.-H.; Lin, Y.-Q.; Sylvestre, A.; Bai, J. High Dielectric Permittivity and Low Percolation Threshold in Polymer Composites Based on Sic-Carbon Nanotubes Micro/Nano Hybrid. *Appl. Phys. Lett.* **2011**, *98* (3), 032901.
(49) Li, W.; He, D.; Dang, Z.; Bai, J. In Situ Damage Sensing in The Glass Fabric Reinforced Epoxy Composites Containing CNT−Al2O3 Hybrids. *Compos. Sci. Technol.* **2014**, *99*, 8−14.
(50) Hu, N.; Karube, Y.; Yan, C.; Masuda, Z.; Fukunaga, H. Tunneling Effect in A Polymer/Carbon Nanotube Nanocomposite Strain Sensor. *Acta Mater.* **2008**, *56* (13), 2929−2936.
(51) Sheng, P. Fluctuation-Induced Tunneling Conduction in Disordered Materials. *Phys. Rev. B* **1980**, *21* (6), 2180−2195.
(52) Castillo-Castro, T.; Castillo-Ortega, M. M.; Encinas, J. C.; Herrera Franco, P. J.; Carrillo-Escalante, H. J. Piezo-resistance Effect in Composite Based on Cross-linked Polydimethylsiloxane and Polyaniline: Potential Pressure Sensor Application. *J. Mater. Sci.* **2011**, *47* (4), 1794−1802.

DOI: 10.1021/acsami.5b01413
ACS Appl. Mater. Interfaces 2015, 7, 9652−9659